ACS APPLIED MATERIALS & INTERFACES

Research Article

www.acsami.org

Multifunctional Janus Hematite–Silica Nanoparticles: Mimicking Peroxidase-Like Activity and Sensitive Colorimetric Detection of Glucose

Chang Lu,[†,‡] Xiangjiang Liu,[‡] Yunfeng Li,[§] Fang Yu,[†] Longhua Tang,*[,†] Yanjie Hu,*[,§] and Yibin Ying*[,‡]

[†]State Key Laboratory of Modern Optical Instrumentation, Department of Optical Engineering and [‡]College of Biosystems Engineering and Food Science, Zhejiang University, Hangzhou 310027, China

[§]Key Laboratory for Ultrafine Materials of Ministry of Education, School of Materials Science and Engineering, East China University of Science and Technology, 130 Meilong Road, Shanghai 200237, China

Supporting Information

ABSTRACT: The design and engineering of multifunctional nanostructures with multiple components and synergistic properties are in urgent demand for variety of acceptable biosensing platforms, enabling users to fulfill multiple tasks in a single nanosystem. Herein, we report using an asymmetric hematite–silica hybrid of Janus γ-Fe_2O_3/SiO_2 nanoparticles (JFSNs) as a multifunctional biosensing platform for sensitive colorimetric detection of H_2O_2 and glucose. It was demonstrated that JFSNs exhibit an intrinsic peroxidase-like catalytic activity. Compared with natural enzyme, JFSNs nanoenzymes could be used over a wider range of pH and temperatures and were more stable over time. Importantly, besides its excellent catalytic activity, the asymmetric properties of the Janus nanoparticle enable it to form the multiple functional utilities for various biosensing applications, including the ease of surface modification without deactivation of catalytic activity and recoverable use by magnetic separation. Thus, we utilized JFSNs with glucose oxidase (GOx) immobilization for glucose-sensitive colorimetric detection, which exhibited both catalytic activity of glucose oxidase and peroxidase with high selectivity and acceptable reproducibility. By combining these two analysis systems into Janus particles, an all-in-one and reusable sensor for blood glucose was formed and has the capability for determination of glucose in complex samples such as serum. These results suggest that such Janus nanosystems have the potential to construct robust nanoarchitecture with multiple functionalities for various biosensing applications.

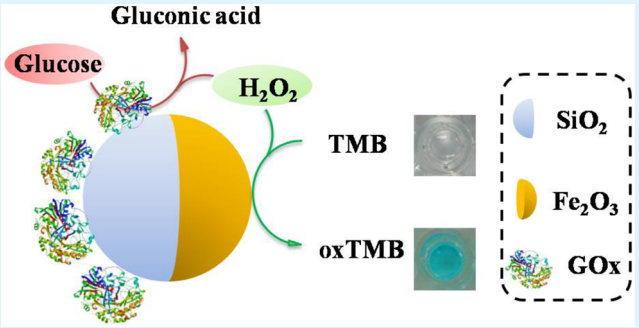

KEYWORDS: *hematite–silica, Janus nanoparticle, colorimetric biosensor, hydrogen peroxide, glucose*

INTRODUCTION

The thrust in (bio)sensor research moves toward systematic assembling of multiple components into a multifunctional utility, enabling simultaneous and rapid detection of a large number of analytes with integrated capabilities of separation and concentration, signal transduction, and quantification.[1] To incorporate the multiple functionalities into a sensing system, much effort has been devoted to understanding and fine-tuning the multicomponent nanostructures, including their material composition and interface engineering.[2] Conceptionally, various existing nanosystems (e.g., TiO_2,[2] CeO_2,[3] Au,[4] Fe_3O_4,[5] and SiO_2[6]) can be structurally and chemically tailored to combine complex properties and functionalities.[7] For example, the noncentrosymmetric coupling of Au and Fe_3O_4 nanoparticles has been reported to potentially generate extremely strong magnetic and enhanced catalytic activity and can be potentially applied as an optical reporter and a magnetic handle for bioassays.[8] However, the current controllable synthesis of these multifunctional nanostructures still faces tremendous challenges, and problems still exist in their biosensing application. One of the major limitations is that the interaction interface of different components may restrict partial properties of each component. For instance, as for core/shell structures, additional coatings and bioconjugation will dramatically decrease their special properties, such as degradation of catalytic activity from the core component. Another significant limitation for commonly used nanosystems with symmetrical geometry is their limited surface available for attaching multiple components, which leads to unfavorable structural and chemical arrangements of these functional components. Therefore, the design and assembly of multiple functional nanostructure with multicomponents and synergistic properties are urgently desired for a variety of acceptable

Received: April 20, 2015
Accepted: June 25, 2015
Published: June 25, 2015

DOI: 10.1021/acsami.5b03423
ACS Appl. Mater. Interfaces 2015, 7, 15395–15402

biosensing platforms, which are expected to best utilize the intrinsic properties of the whole nanosystem.

Recently, "Janus"-type nanoparticles, named after the double-faced Roman god Janus, have emerged as a new division of multifunctional nanocomposites.[9] Such asymmetric architectures are composed of two incompatible hemispheres with different chemistry, polarity, or other physicochemical properties on opposite sides.[10,11] Although Janus nanoparticles combine individual components together, the intrinsic optical, magnetic, and electronic properties of each component are not often altered, interfered with, or completely lost,[12] thereby exhibiting improved physical/chemical properties[13] and great potential in numerous applications.[14] This makes them a unique category of materials in contrast to other particles. Specifically, the ease of functional modification on the distinct surface, which is the key step for the utilization of nanosystems in the field of biosensor and other bionanotechnology, renders Janus nanoparticles truly multifunctional entities. To date, a variety of Janus nanoparticles have been reported as synthesized for applications in (bio)sensing,[14] magnetic fluorescent display or imaging,[15] and drug delivery.[16] However, only a few studies explored the potential of these Janus nanoparticles for multifunctional biosensing applications that simultaneously achieve separation and concentration, signal transduction, and rapid and sensitive detection.

In contrast, the development of nanobiosensors for sensitive and rapid glucose monitoring is in great demand because of the subjects with diabetes mellitus, which represents one of the largest health concerns of the 21st century with worldwide prevalence.[17,18] Among all these analytical techniques, the colorimetric biosensing method has received considerable attention owing to its simplicity, improved sensitivity, and high selectivity. Moreover, through this method, changes can be read out directly by the naked eye. No expensive or sophisticated instrumentation is required, and it may be applied in field analysis and clinical and point-of-care (POC) diagnosis.[19] In the past few years, it has been found that some enzyme-like nanomaterials, such as Fe_3O_4 and Au nanoparticles, can catalyze the reaction of the peroxidase substrate to produce a color change,[20−23] which affords an important tool for glucose colorimetric biosensing. Moreover, these enzyme-like nanomaterials show several advantages over natural enzymes, such as controlled synthesis at a low cost, tunability in catalytic activities, and high stability against stringent conditions, thus being used in various aspects.[24−30] Particularly, magnetic nanoparticles (MNPs) have been considered as one of the most important nanozymes because of their unique peroxidase-like activity, magnetic, nontoxic, and highly biocompatible properties, and potential applications in biological separation,[31] drug delivery,[32] and biological catalysis.[33] Unfortunately, there is still a challenging problem for the use of peroxidase-like MNPs nanozyme in glucose colorimetric detection because the surface modification (e.g., glucose oxidase) and additional coatings (e.g., SiO_2) can decrease the peroxidase activity dramatically.[20] Thus, novel surface structure and bioconjugation techniques are required to maximize the performance of nanozymes. Moreover, to offer multiple functions in response to the glucose, exploring or developing multifunctional enzyme mimetics with high sensitivity, catalytic activity, reusability, stability, and low toxicity still requires further efforts.

In the present report, we describe a multifunctional hybrid Janus nanoparticles that are designed for colorimetric detection of glucose, which are a new kind of multifunctional nanozyme with peroxidase-like activity, and explored their biosensing application of H_2O_2 and glucose detection, as schematically illustrated in Scheme 1. According to our previous report,[34] we designed and synthesized a unique spherical Janus nanoparticles composed of γ-Fe_2O_3 and SiO_2. Interestingly, we here found that the resultant Janus hematite nanoparticles exhibit excellent peroxidase-like activity as well as magnetism functions for separation and concentration.[35] Moreover, the existence of SiO_2 in the Janus nanoparticle facilitates the surface modification and bioconjugation of the particles.[36] Importantly, because of their asymmetric structure, such Janus nanoparticles will not suffer from inertness toward bioconjugation and render multiple functions. Therefore, we immobilized glucose oxidase (GOx) onto the Janus nanoparticle to prepare bioactive, magnetic peroxidase-like nanozymes for glucose colorimetric sensing. It was demonstrated that the GOx-attached Janus nanoparticles have both glucose oxidase like and peroxidase-like activity, resulting in fast and sensitive detection of glucose in one system. Meanwhile, because of its magnetic nature, the Janus-nanoparticles-based sensing platform permits easy sample separation/concentration, recycling, and reuse[37] as well as allowing the multiple detection of glucose in a complex sample such as serum.

Scheme 1. Schematic Illustration of the Peroxidase-Like Activity of JFSNs in Catalysis of the TMB−H_2O_2 System and Using GOx-JFSNs as Biosensing Platform for Colorimetric Detection of H_2O_2 and Glucose[a]

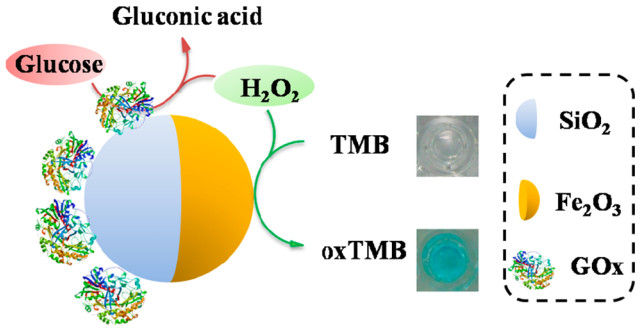

[a]Pictures present the color change of TMB before and after the catalytic reaction.

EXPERIMENTAL SECTION

Chemicals and Materials. Horseradish peroxidase (HRP, 25000 IU/mg), glucose oxidase (GOx, from *Aspergillus niger*), 30% H_2O_2, and 3,3′,5,5′-tetramethylbenzidine (TMB) were obtained from Sigma-Aldrich (Beijing, China). Glucose, maltose, *R*-lactose, and D-fructose were purchased from Beijing Chemical Reagent Factory (Beijing, China). All other chemicals were analytical-grade and used without further purification. All aqueous solutions were prepared with Milli-Q water (>18.3 MΩ cm). The JFSNs were synthesized by a one-step flame-assisted spray-pyrolysis (FASP) approach using an enclosed reactor according to previous methods.[34]

JFSNs Modification with GOx. The JFSNs (40 mg) were first introduced into 20 mL of isopropanol solution (2 mg mL^{-1}). The resultant suspension was ultrasonicated for 30 min, and then 100 μL of (3-aminopropyl) triethoxysilane was added to the solution. After reaction under stirring for 12 h, the Janus magnetic nanoparticles was separated by magnetic force and then washed by ethanol and distilled water several times. Finally, the sample was redispersed in water (16 mL) and stored at 4 °C, being referred to as amine−JFSNs solution.

DOI: 10.1021/acsami.5b03423
ACS Appl. Mater. Interfaces 2015, 7, 15395−15402

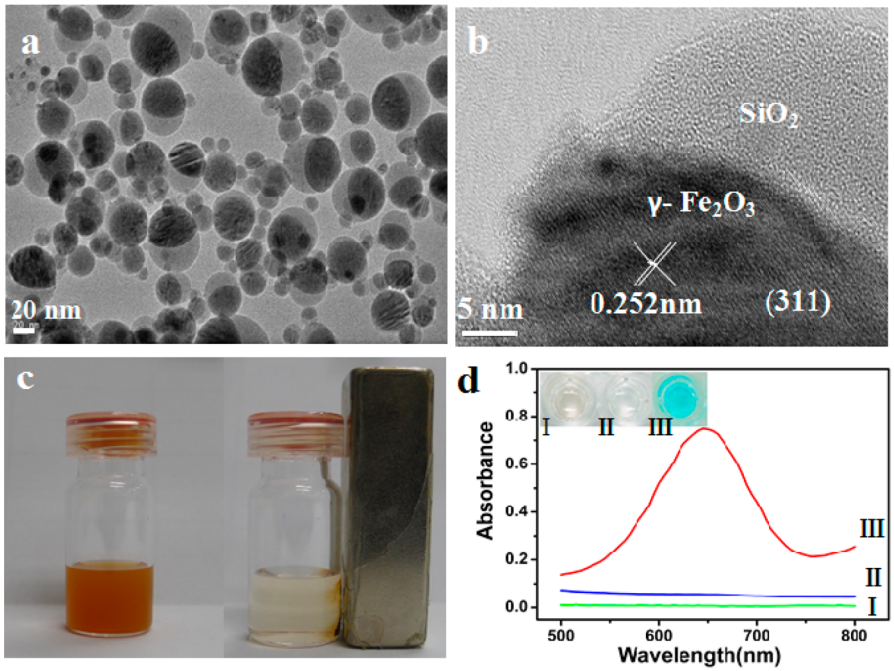

Figure 1. (a) Low- and (b) high-resolution TEM images of JFSNs. (c) Photograph of JFSNs dispersed in water (left) and their response to the external magnetic field (right). (d) Typical absorption spectra of TMB–H_2O_2 mixed solution in the absence and presence of JFSNs: (I) TMB + JFSNs, (II) TMB + H_2O_2, and (III) TMB + H_2O_2 + JFSNs. Photograph of the solutions shown in the inset. [TMB] = 510 μM; [H_2O_2] = 1.59M; [JFSNs] = 0.06 mg mL^{-1}; reaction buffer: potassium citrate buffer (0.1 M, pH 3.7); incubation temperature = 30 °C; reaction time = 10 min.

Then, 12 mL of the resultant amine–JFSNs solution was treated with 4 mL of 2% glutaraldehyde in 4 mL of PBS solution (pH 7.4) at 25 °C for 2 h. After washing by distilled water, the resulted nanoparticles were dispersed in 2 mL of PBS buffer solution (pH 6.0) containing 400 μL of 1.0 mg mL^{-1} GOx. The mixture was incubated for reaction under shaking for 12 h at 25 °C. After removing the unbound enzyme by a separation and washing process, the GOx-immobilized γ-Fe_2O_3/SiO_2 Janus NP, referred to as GOx-JFSNs, were obtained.

JFSNs Catalytic Study. The catalytic activities of JFSNs for oxidation of TMB in the presence of H_2O_2 were investigated using the following procedures: JFSNs (60 μg mL^{-1}) were incubated with 100 μL of potassium citrate buffer (0.1 M, pH 3.7) solution containing 510 mM TMB (freshly prepared) and 1.59 M H_2O_2. After the mixed solution was incubated at 30 °C for 10 min, photographs and UV spectra of the mixtures were taken. The catalytic activity of HRP was also tested by incubation with 2 ng mL^{-1} HRP, 816 μM TMB, and 8.8 mM H_2O_2.

To analyze the reaction kinetics, steady-state kinetics assays of JFSNs toward TMB oxidation were carried out with varied concentrations of the substrate TMB or H_2O_2 at room temperature. Unless otherwise stated, the concentrations of TMB and H_2O_2 were the same as those used above. The absorbance variation of the reaction solution was monitored in time-scan mode at 652 nm.[38] The kinetic parameters of the catalytic reaction were determined on the basis of the Michaelis–Menten function, $v = V_{max}[S]/(K_m + [S])$, where v is the initial velocity of the reaction, V_{max} is the maximal rate of reaction, [S] is the substrate concentration, and K_m is the Michaelis–Menten constant, which is equivalent to the substrate concentration at which the rate of conversion is half of V_{max} and denotes the affinity of the enzyme.[39] V_{max} was calculated into molar change from UV absorbance on the basis of the equation of $A = \varepsilon lc$ (where A is the absorbance, ε is the absorbance coefficient, l is the path length, and c is the molar concentration) with $\varepsilon = 3.9 \times 10^4$ M^{-1} cm^{-1} and $l = 10$ mm.[40]

To study the influence of reaction buffer pH on the relative activity of JFSNs and HRP, 0.1 M potassium citrate buffer solutions (pH 1.0–12.0) were used. To examine the influence of incubation temperature on the relative activity of JFSNs and HRP, catalytic reactions were incubated from 30 to 60 °C under identical conditions. To investigate the stability of peroxidase-like activity, JFSNs and HRP were stored at room temperature, and the catalytic activity was measured every 24 h for consecutive 7 days.

Colorimetric Detection of H_2O_2. H_2O_2 was tested as follows: 0.625 μL of TMB (81.6 mM), 0.2 mg of as-prepared JFSNs, and 10 μL of H_2O_2 with various concentrations were added into 90 μL of potassium citrate buffer (0.1 M, pH 3.7). Then, the mixed solution was measured by UV–vis absorption spectroscopy.

Glucose Detection. A reaction solution of 50 μL of GOx-JFSNs solution and 50 μL of glucose with different concentrations in PBS (pH 7.0) were incubated at 37 °C for 1 h. Then, 1.25 μL of 81.6 mM TMB and 100 μL of potassium citrate buffer (pH 3.7) were added to the above 100 μL of reaction solution. After incubation for 15 min, GOx-JFSNs were removed from the reaction solution by an external magnetic field. Subsequently, the final reaction solution was used for adsorption spectroscopy measurement. We also used fetal bovine serum as the model to verify the capability of detection in complex samples. Glucose was measured in the serum-containing PBS solution (pH 7.0).

Characterizations. High-resolution transmission electron microscopy (HRTEM; JEM- 2010, operated at 200 kV) and low-resolution transmission electron microscopy (TEM, H-800) were used to characterize the morphology microstructure. X-ray diffraction (XRD, Rigaku D/max 2550VB/PC diffractometer with Cu Kα radiation) and energy-dispersive X-ray spectroscopy (EDS, JEM-2010) were employed to obtain chemical composition and structure information on flame-made NPs. The absorption and reaction kinetics were measured via UV–vis spectrometry (Thermofisher Evolution 201).

RESULTS AND DISCUSSION

In this study, the asymmetric hematite–silica nanoparticles of Janus γ-Fe_2O_3/SiO_2 nanoparticles, denoted as JFSNs, were synthesized using a FASP approach according to our previous report.[34] As shown in the TEM images (Figure 1a,b), the obtained nanoparticles have a typical asymmetric Janus-type morphology with ~20–120 nm diameters. Each particle is composed of two distinct hemispheres, and an obvious

DOI: 10.1021/acsami.5b03423
ACS Appl. Mater. Interfaces 2015, 7, 15395–15402

interface can be viewed between them. The HRTEM images (Figure 1b) also revealed that the interplanar spacing of the lattice fringes of the dark hemisphere is about 0.252 nm, which is in good agreement with the interpalnar distance of γ-Fe_2O_3 phase.[41] In contrast, the other light hemisphere presented the amorphous nature of silica oxide. Furthermore, the constituents and crystal phases of as-prepared nanoparticles were confirmed by EDS and XRD. According to EDS and XRD results, the as-prepared nanoparticles showed the typical γ-Fe_2O_3 and SiO_2 signals, suggesting the successful synthesis of JFSNs nanohybrids (Figure S1a,b, Supporting Information). In addition, the as-prepared nanoparticles can be well dispersed in aqueous solution (Figure 1c, left) and remain stable for more than 12 h without noticing any aggregation (verified by UV−vis spectra; no detectable change occurred overnight). We also tested the magnetic response of the obtained JFSNs. When the JFSNs suspension solution was exposed to the external magnetic field, it was observed that the brown nanoparticles could be quickly attracted by an external magnet (Figure 1c). Meanwhile, the room-temperature magnetization result proved that the JFSNs have a good magnetic response with a saturated magnetization at 22.5 emu g^{-1} (Figure S1c, Supporting Information). This magnetic nature of JFSNs suggests their potential applications in magnetic resonance imaging (MRI), magnetic targeting, and hyperthermia. All together, these results demonstrated that the successful synthesis of the JFSNs.

To investigate the peroxidase-like activity of JFSNs, the catalysis of the chromogenic peroxidase substrate TMB was tested in the presence of H_2O_2. As shown in Figure 1d, the as-prepared JFSNs produced a blue color in the presence of H_2O_2 and TMB, indicating that the nanoparticles can catalyze the oxidation of TMB. The corresponding absorption spectra are shown in Figure 1d, in which the absorbance peak localized at 652 nm originates from the oxidation of TMB.[38] The possible reaction mechanism involves two cascade steps as investigated elsewhere:[40] First, H_2O_2 was adsorbed onto the surface of JFSNs, and the O−O bond was broken into ·OH. Second, TMB was oxidized by ·OH to form a blue-colored product. Additional control experiments using TMB in the absence of JFSNs or H_2O_2 show no appearance of the oxidation peak of the TMB, indicating that both the components are required for the reaction, as is also the case with horseradish peroxidase (HRP). Moreover, it is found that the TMB oxidation catalyzed by the γ-Fe_2O_3/SiO_2 is dependent on the concentration of JFSNs (Figure S2, Supporting Information). Also, TEM imaging illustrated that the morphology and phase of the γ-Fe_2O_3/SiO_2 nanoparticles after the peroxidase reaction remained unchanged (Figure S3, Supporting Information). All these results confirm that the JFSNs exhibit an intrinsic peroxidase-like activity.

To better understand the mechanism of the peroxidase-like catalytic activity of JFSNs, we analyzed the steady-state kinetics for TMB oxidation reaction compared to those of horseradish peroxidase (HRP) at neutral pH. The kinetic data were obtained by varying one substrate concentration while keeping the other substrate concentration constant. Under the optimum conditions (details in the Supporting Information), a series of initial reaction rates were calculated and applied to the double reciprocal of the Michaelis−Menten equation.[39] From the Lineweaver−Burk plot, the key enzyme kinetic parameters such as maximum initial velocity (V_{max}) and Michaelis−Menten constant (K_m) were obtained and are given in Table 1. It is observed that the oxidation reaction catalyzed by the JFSNs (Figure 2a,b) and HRP (Figure 2c,d) follows the typical Michaelis−Menten model toward both substrates, TMB and H_2O_2, so we can use the Michaelis−Menten model to evaluate the catalysis of JFSNs and HRP. The V_{max} value is a direct measure of the enzymatic catalytic activity. K_m is identified as an indicator of enzyme affinity to substrates. A low K_m represents a high affinity and vice versa.[42] The reaction rate obtained from JFSNs had a significant increase at low TMB concentration (<0.612 mM) and reaches V_{max} when TMB exceeds 0.612 mM. In contrast, the reaction from HRP is much slower. The V_{max} of JFSNs is nearly twice that with HRP when TMB was used as substrate, whereas the apparent K_m value of JFSNs with substrate H_2O_2 was significantly higher than that for HRP, which is in agreement with the observation that a higher H_2O_2 concentration was required to achieve maximal activity for JFSNs. The apparent K_m value of JFSNs with TMB as the substrate was lower than that of HRP, suggesting that JFSNs have a higher affinity for TMB. These results indicate that JFSNs exhibit peroxidase-like activity toward typical peroxidase substrates. This may be due to the existence of more "active sites" on the nanosized surface of the Janus particles compared to HRP, which has only one iron ion at the active center. It is worthwhile to point out that because JFSNs-based catalysis is a complicated reaction with multiple active sites for TMB oxidation and possibly able to support multiple reactions simultaneously, the classic Michaelis−Menten equation cannot precisely describe this reaction. The other reactions are, nevertheless, at a much smaller level than JFSNs-based catalysis. However, this equation is still employed because it provides a simple measurement for comparison of kinetics.[21]

Table 1. Comparison of the Apparent Michaelis−Menten Constant (K_m) and Maximum Reaction Rate (V_{max}) of JFSNs and HRP

substrate	catalyst	K_m (mM)	V_{max} (mM min^{-1})
TMB	JFSNs	3.05	0.25
TMB	HRP	5.90	0.11
H_2O_2	JFSNs	965.98	769.65
H_2O_2	HRP	0.63	1.35

It is known that the catalytic activity of natural enzyme or nanoenzyme is dependent on pH and temperature.[43] In accordance with the previous reports,[27] HRP was largely inhibited after incubation at either lower or higher pH or higher temperature. As a kind of inorganic nanomaterial, JFSNs are expected to function in a wider range of pH and temperature than HRP. To prove this, varied reaction conditions with a range of values of pH (1−12) or temperature (30−60 °C) were used to investigate the catalytic activity of JFSNs. For comparison, the catalytic activity of natural enzyme HRP was tested under same conditions. As shown in Figure 3a, the pH-dependent response of the catalytic activity of the JFSNs remained stable over a wider pH range (pH 2−5). In contrast, HRP was largely inhibited when pH was either lower than 4 or higher than 5. As shown in Figure 3b, the catalytic activity of JFSNs was less sensitive to temperature than HPR. The JFSNs preserved a high activity between 30−55 °C, whereas the activity of HRP dramatically decreased when the temperature exceeded 30 °C. These results indicated that the catalytic activity of the JFSNs remained stable over wide temperature and pH ranges. Notably, the JFSNs can properly operate at a near-neutral pH, which would open up various potential applications of this catalytic system in biological systems.

DOI: 10.1021/acsami.5b03423
ACS Appl. Mater. Interfaces 2015, 7, 15395−15402

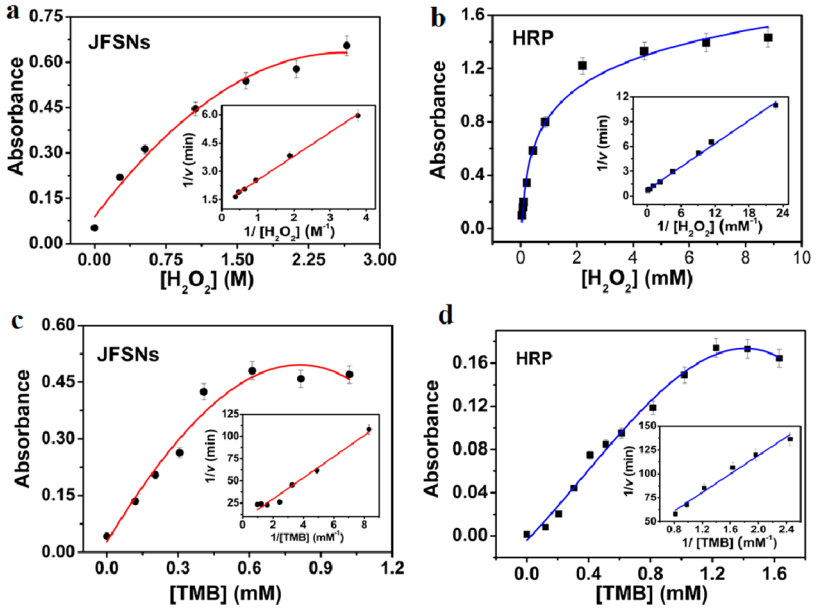

Figure 2. Steady-state kinetic assays of the JFSNs and HRP. (a and b) The concentration of TMB was fixed (510 μM JFSNs and 816 μM HRP), and H_2O_2 concentration was varied. (c and d) The concentration of H_2O_2 was fixed (1.5 M JFSNs and 8.8 mM HRP), and TMB concentration was varied. Insets are the Lineweaver–Burk plots of the double reciprocal of the Michaelis–Menten equation.

Furthermore, the storage stability, i.e., the ability of enzyme to maintain activity over a long period of time, is an important aspect to be considered in practical applications. To evaluate the catalytic activity stability of the JFSNs with long-term storage, the same batch of JFSNs nanoparticles was measured with the same analytical operation over 7 days. HRP was chosen as the comparison enzyme, which was stored at room temperature when not in use. As shown in Figure 3c, the peroxidase-like activity of JFSNs remained intact over 7 days, exhibiting good stability. In contrast, the activity of HRP decreased significantly, which is consistent with the fact that HRP has low stability and is easily deactivated in surrounding environments. Thus, JFSNs, as HRP mimics, behave insensitively to ambient conditions and keep excellent catalytic activity.

To sum up, the JFSNs exhibit high and stable peroxidase-like activity toward H_2O_2 over a wide rage of pH and temperature. Accordingly, direct quantitative colorimetric detection of H_2O_2 on the basis of such peroxidase-like activity of JFSNs can be achieved. In the presence of TMB (0.625 M TMB) and different concentrations of H_2O_2, the JFSNs could catalyze a color reaction that could be monitoried either by the naked eye or by the absorbance change at 652 nm. Figure S4a (Supporting Information) showed absorbance changes in the presence of different concentrations of H_2O_2. A color change of the reaction solution could be observed when the H_2O_2 concentration was above 200 μM (Figure S4b, inset) indicating oxidation of TMB. A linear range from 1–100 μM and limit of detection (LOD) of 10.6 nM can be achieved (LOD = $3\sigma/k$, where σ is the standard deviation of the blank sample and k is the slope of the analytical calibration). To the best of our knowledge, this is one of the most sensitive H_2O_2 sensors, which is 1–100-fold more sensitive than previous colorimetric detection.[20,38]

Because the SiO_2 on the other side of JFSNs could be used for surface modification and bioconjugation, JFSNs can be rendered a mutifunctional sensing platform. Here we chose to immobilize glucose oxidase (GOx) on the surface of JFSNs (GOx-JFSNs) for glucose sensing. To evaluate whether the surface modification would influence the catalytic activity of JFSNs, the peroxidase-like activities of JFSNs before and after modification were measured (at 30 °C, 0.1 M potassium citrate buffer, pH 3.7). As shown in Figure S5 (Supporting Information), hardly any difference could be observed after the modification steps, indicating that the attachment of GOx on JFSNs exerts little influence on the catalytic activity. Therefore, it is believed that JFSNs is an ideal multifunctional platform for biosensing applications. It is known that H_2O_2 is the main product of the GOx-catalyzed reaction; therefore, a colorimetric quantitative test of glucose can also be realized using JFSNs instead of traditionally used HRP. Because of the low stability of GOx in pH 3.7 buffer solution, glucose detection was performed in two separated steps. GOx first catalyzes oxidation of the glucose to the products gluconic acid and H_2O_2 in a pH 7.0 buffer solution. Subsequently, the resulted H_2O_2 is reduced in situ by JFSNs in the presence of TMB cosubstrate at pH 3.7, generating a detectable signal. The detailed protocols are described in the Experimental Section. Figure 4 shows a typical glucose-concentration response absorption profile. By varying the glucose concentration, a linear response (0–20 μM) was observed with a detection limit of 3.2 μM glucose (Figure 4, inset b). Moreover, as the glucose concentration increased above 100 μM, the blue color variation can also be observed directly by the naked eye (Figure 4, inset a). Because the ranges for the serum glucose concentrations in healthy and diabetic individuals are 3–8 mM and 9–40 mM, respectively,[44] our biosensor with an LOD of 3.2 μM should normally be sufficient for detection of glucose in blood.

Selectivity is another major concern one in analysis. As shown in Figure 5, the reaction is highly specific to glucose. Even though the concentrations of control samples (fructose, lactose, and maltose) were fivefold higher (5 mM) than that of glucose, the absorbance at 652 nm remained as low as the background. In contrast, for glucose, the resulting blue color can be distinguished directly by the naked eye. This indicates the high selectivity of the GOx-JFSNs for glucose analysis. To

DOI: 10.1021/acsami.5b03423
ACS Appl. Mater. Interfaces 2015, 7, 15395–15402

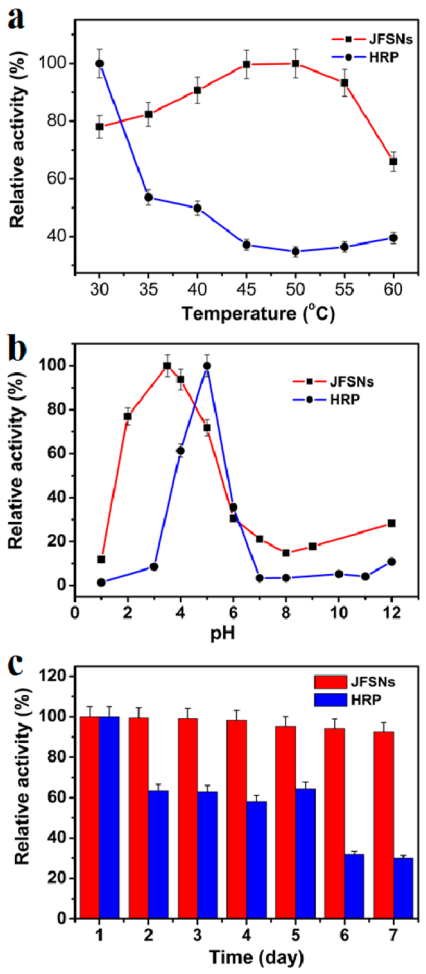

Figure 3. Comparison of the stability of JFSNs and HRP. Peroxidase activities of JFSNs and HRP were measured at (a) pH 1−12 or (b) 30−60 °C under standard conditions. (c) Long-term stability of JFSNs and HRP stored at room temperature. Peroxidase activities were measured at pH 3.7 and 30 °C under standard conditions. Standard conditions were as follows: Experiments were carried out using 0.06 mg mL^{-1} JFSNs in 100 μL of potassium citrate buffer with 510 μM TMB and 1.59 M H_2O_2 as a substrate or 1 ng mL^{-1} HRP in 100 μL of potassium citrate buffer with 816 μM TMB and 8.8 mM H_2O_2 as a substrate. The maximum point in each curve (a−c) was set as 100%.

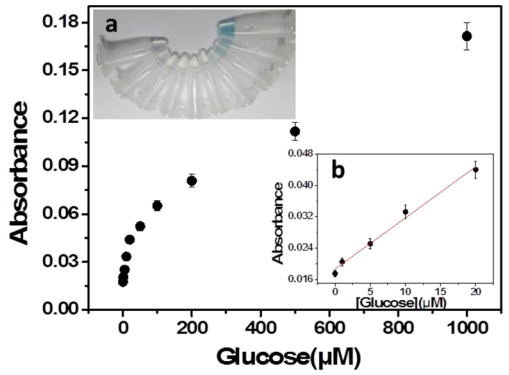

Figure 4. Dose−response curves for glucose detection using JFSNs as peroxidase mimic. Dependence of the absorbance at 652 nm on the concentration of glucose in the range from 0 to 1 mM. Insets: photograph (inset a) shows the production of colored products for different concentrations of glucose and figure (inset b) shows the corresponding linear calibration plots. The error bars represent the standard deviation of the three measurements.

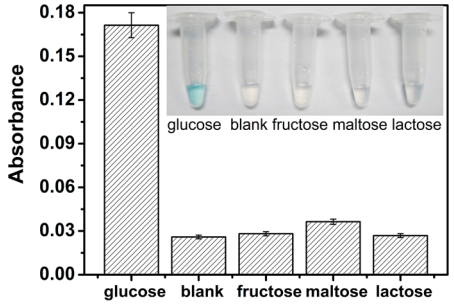

Figure 5. Determination of the selectivity of glucose detection with 1 mM glucose, no saccharide, 5 mM fructose lactose, 5 mM maltose, and 5 mM lactose. Inset: photograph showing colorimetric responses of the system.

further demonstrate the sensing capability in the real sample, we tested glucose in serum (fetal bovine serum as serum model), using a standard addition method. As shown in Figure 6a, we compared the catalytic response of GOx-attached to a JFSNs-based sensor to 50 μM glucose in different serum concentrations. The results indicate that serum had scarce influence on the catalytic activity of the nanocomposite, suggesting that a JFSNs sensing platform may allow for monitoring glucose in complex samples, such as the blood samples of diabetic patients.

Additionally, because of its magnetic properties, JFSNs may offer the additional advantages of JFSNs-based biosensors of recylability and resusability. We investigated the possibility of GOx-JFSNs for reapeated use in glucose measurements. After each measurement, the JFSNs nanoparticles were magnetically separated, washed with a buffer solution and then reused for glucose testing. As shown in Figure 6b, only a slight decrease in the absorbance at 652 nm was observed after five cycles, which might be caused by seldom loss of the GOx-JFSNs in the magnetic separatation procedure or slight degrading of the activity during successive experiments. The above results highly suggest the reusability of the GOx-JFSNs.

CONCLUSIONS

We reported asymmetric hematite−silica nanocomposites (JFSNs) as multifunctional peroxidase mimetics and investigated their applications for colorimetric biosensing. The obtained results indicate that JFSNs exhibit intrinsic peroxidase-like activity, which compared with that of natural enzyme HRP, is higher and more stable over a wide range of pH and temperature values. Furthermore, the as-prepared JFSNs offer a multiple function platform for biosensing because of their unique asymmetric structure. Thus, we demonstrated that JFSNs can be used as a robust analytical platform for glucose colorimetric biosensing through bioconjugated enzyme GOx, providing sensitive and selective colorimetric assay for glucose. The results suggest the good reproducibility and long-term stability of GOx-JFSNs, which make JFSNs a promising candidate for peroxidase and glucose oxidase mimics for bioassays and medical diagnostics. Therefore, it is believed that the coupling Janus architecture can pave a way for the fabrication of multifunctional nanocomposites with higher performance in biosensing, adsorption, and catalysis and separation, among others.

DOI: 10.1021/acsami.5b03423
ACS Appl. Mater. Interfaces 2015, 7, 15395−15402

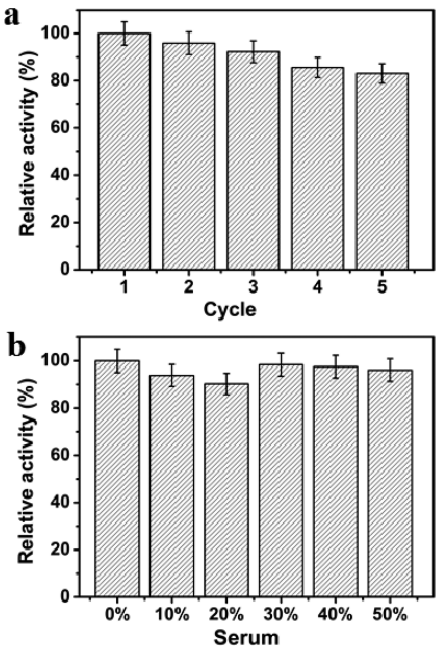

Figure 6. (a) Reusability of JFSNs after repeated cycles of glucose sensing using identical reaction conditions. (b) Catalytic activity of 50 μM glucose in buffer and in 10−50% fetal bovine serum. The maximum point in each curve was set as 100%. Here, we used relative activity to present the catalytic activity.

■ ASSOCIATED CONTENT

Supporting Information

Characterization of the as-synthesized JFSNs. Influence of concentrations of JFSNs on the catalytic reaction. TEM image of JFSNs after the catalytic reaction. Absorbance changes in the presence of different concentrations of H_2O_2. Influence of modification of JFSNs on the catalytic activity. The Supporting Information is available free of charge on the ACS Publications website at DOI: 10.1021/acsami.5b03423.

■ AUTHOR INFORMATION

Corresponding Authors

*E-mail: lhtang@zju.edu.cn.
*E-mail: huyanjie@ecust.edu.cn.
*E-mail: ibeying@zju.edu.cn.

Author Contributions

C.L. and X.L. contributed equally to this work.

Notes

The authors declare no competing financial interest.

■ ACKNOWLEDGMENTS

This work was financially supported by National Natural Science Foundation of China (21305125, 61405176), Zhejiang Educational Committee (Y201225865), Natural Sciences Fund of Zhejiang Province (LY14B050004), and the Fundamental Research Funds for the Central Universities.

■ REFERENCES

(1) Schrinner, M.; Proch, S.; Mei, Y.; Kempe, R.; Miyajima, N.; Ballauff, M. Stable Bimetallic Gold−Platinum Nanoparticles Immobilized on Spherical Polyelectrolyte Brushes: Synthesis, Characterization, and Application for the Oxidation of Alcohols. *Adv. Mater.* **2008**, *20*, 1928−1933.

(2) Seh, Z. W.; Liu, S.; Low, M.; Zhang, S. Y.; Liu, Z.; Mlayah, A.; Han, M. Y. Janus Au-TiO_2 Photocatalysts with Strong Localization of Plasmonic Near-Fields for Efficient Visible-Light Hydrogen Generation. *Adv. Mater.* **2012**, *24*, 2310−2314.

(3) Cargnello, M.; Wieder, N. L.; Montini, T.; Gorte, R. J.; Fornasiero, P. Synthesis of Dispersible Pd@ CeO_2 Core− Shell Nanostructures by Self-Assembly. *J. Am. Chem. Soc.* **2010**, *132*, 1402−1409.

(4) Xu, C.; Xie, J.; Ho, D.; Wang, C.; Kohler, N.; Walsh, E. G.; Morgan, J. R.; Chin, Y. E.; Sun, S. Au−Fe_3O_4 Dumbbell Nanoparticles as Dual-Functional Probes. *Angew. Chem., Int. Ed.* **2008**, *47*, 173−176.

(5) Jin, Y.; Jia, C.; Huang, S.-W.; O'Donnell, M.; Gao, X. Multifunctional Nanoparticles as Coupled Contrast Agents. *Nat. Commun.* **2010**, *1*, 1.

(6) Nann, T.; Mulvaney, P. Single Quantum Dots in Spherical Silica Particles. *Angew. Chem., Int. Ed.* **2004**, *43*, 5393−5396.

(7) Zeng, H.; Sun, S. Syntheses, Properties, and Potential Applications of Multicomponent Magnetic Nanoparticles. *Adv. Funct. Mater.* **2008**, *18*, 391−400.

(8) Lee, Y.; Garcia, M. A.; Frey Huls, N. A.; Sun, S. Synthetic Tuning of the Catalytic Properties of Au-Fe_3O_4 Nanoparticles. *Angew. Chem.* **2010**, *122*, 1293−1296.

(9) Hu, J.; Zhou, S.; Sun, Y.; Fang, X.; Wu, L. Fabrication, Properties and Applications of Janus Particles. *Chem. Soc. Rev.* **2012**, *41*, 4356−4378.

(10) Glotzer, S. C.; Solomon, M. J. Anisotropy of Building Blocks and Their Assembly into Complex Structures. *Nat. Mater.* **2007**, *6*, 557−562.

(11) Ling, X. Y.; Phang, I. Y.; Acikgoz, C.; Yilmaz, M. D.; Hempenius, M. A.; Vancso, G. J.; Huskens, J. Janus Particles with Controllable Patchiness and their Chemical Functionalization and Supramolecular Assembly. *Angew. Chem.* **2009**, *121*, 7813−7818.

(12) Jin, Y.; Gao, X. Plasmonic Fluorescent Quantum Dots. *Nat. Nanotechnol.* **2009**, *4*, 571−576.

(13) Xu, C.; Wang, B.; Sun, S. Dumbbell-like Au− Fe_3O_4 Nanoparticles for Target-Specific Platin Delivery. *J. Am. Chem. Soc.* **2009**, *131*, 4216−4217.

(14) Walther, A.; Müller, A. H. Janus Particles: Synthesis, Self-Assembly, Physical Properties, and Applications. *Chem. Rev.* **2013**, *113*, 5194−5261.

(15) Yin, S. N.; Wang, C. F.; Yu, Z. Y.; Wang, J.; Liu, S. S.; Chen, S. Versatile Bifunctional Magnetic-Fluorescent Responsive Janus Supraballs Towards the Flexible Bead Display. *Adv. Mater.* **2011**, *23*, 2915−2919.

(16) Percec, V.; Wilson, D. A.; Leowanawat, P.; Wilson, C. J.; Hughes, A. D.; Kaucher, M. S.; Hammer, D. A.; Levine, D. H.; Kim, A. J.; Bates, F. S.; et al. Self-Assembly of Janus Dendrimers into Uniform Dendrimersomes and Other Complex Architectures. *Science* **2010**, *328*, 1009−1014.

(17) Bao, S. J.; Li, C. M.; Zang, J. F.; Cui, X. Q.; Qiao, Y.; Guo, J. New Nanostructured TiO_2 for Direct Electrochemistry and Glucose Sensor Applications. *Adv. Funct. Mater.* **2008**, *18*, 591−599.

(18) Liu, B.; Sun, Z.; Huang, P. J.; Liu, J. Hydrogen Peroxide Displacing DNA from Nanoceria: Mechanism and Detection of Glucose in Serum. *J. Am. Chem. Soc.* **2015**, *137*, 1290−1295.

(19) Bonanno, L. M.; DeLouise, L. A. Integration of a Chemical-Responsive Hydrogel into a Porous Silicon Photonic Sensor for Visual Colorimetric Readout. *Adv. Funct. Mater.* **2010**, *20*, 573−578.

(20) Gao, L.; Zhuang, J.; Nie, L.; Zhang, J.; Zhang, Y.; Gu, N.; Wang, T.; Feng, J.; Yang, D.; Perrett, S.; et al. Intrinsic Peroxidase-like Activity of Ferromagnetic Nanoparticles. *Nat. Nanotechnol.* **2007**, *2*, 577−583.

(21) Zheng, X.; Liu, Q.; Jing, C.; Li, Y.; Li, D.; Luo, W.; Wen, Y.; He, Y.; Huang, Q.; Long, Y. T.; Fan, C. Catalytic Gold Nanoparticles for Nanoplasmonic Detection of DNA Hybridization. *Angew. Chem., Int. Ed.* **2011**, *50*, 11994−11998.

(22) Li, K.; Wang, K.; Qin, W.; Deng, S.; Li, D.; Shi, J.; Huang, Q.; Fan, C. DNA-Directed Assembly of Gold Nanohalo for Quantitative

DOI: 10.1021/acsami.5b03423
ACS Appl. Mater. Interfaces 2015, 7, 15395−15402

Plasmonic Imaging of Single-Particle Catalysis. *J. Am. Chem. Soc.* **2015**, *137*, 4292−4295.
(23) Luo, W.; Zhu, C.; Su, S.; Li, D.; He, Y.; Huang, Q.; Fan, C. Self-Catalyzed, Self-Limiting Growth of Glucose Oxidase-Mimicking Gold Nanoparticles. *ACS Nano* **2010**, *4*, 7451−7458.
(24) Zhang, X.-Q.; Gong, S.-W.; Zhang, Y.; Yang, T.; Wang, C.-Y.; Gu, N. Prussian Blue Modified Iron Oxide Magnetic Nanoparticles and their High Peroxidase-like Activity. *J. Mater. Chem.* **2010**, *20*, 5110−5116.
(25) Wei, H.; Wang, E. Nanomaterials with Enzyme-Like Characteristics (Nanozymes): Next-Generation Artificial Enzymes. *Chem. Soc. Rev.* **2013**, *42*, 6060−6093.
(26) Song, S.; Qin, Y.; He, Y.; Huang, Q.; Fan, C.; Chen, H.-Y. Functional Nanoprobes for Ultrasensitive Detection of Biomolecules. *Chem. Soc. Rev.* **2010**, *39*, 4234−4243.
(27) Song, Y.; Qu, K.; Zhao, C.; Ren, J.; Qu, X. Graphene Oxide: Intrinsic Peroxidase Catalytic Activity and its Application to Glucose Detection. *Adv. Mater.* **2010**, *22*, 2206−2210.
(28) Cui, R.; Han, Z.; Zhu, J. J. Helical Carbon Nanotubes: Intrinsic Peroxidase Catalytic Activity and its Application for Biocatalysis and Biosensing. *Chem. - Eur. J.* **2011**, *17*, 9377−9384.
(29) He, W.; Wu, X.; Liu, J.; Hu, X.; Zhang, K.; Hou, S.; Zhou, W.; Xie, S. Design of AgM Bimetallic Alloy Nanostructures (M= Au, Pd, Pt) with Tunable Morphology and Peroxidase-like Activity. *Chem. Mater.* **2010**, *22*, 2988−2994.
(30) André, R.; Natálio, F.; Humanes, M.; Leppin, J.; Heinze, K.; Wever, R.; Schröder, H. C.; Müller, W. E.; Tremel, W. V_2O_5 Nanowires with an Intrinsic Peroxidase-Like Activity. *Adv. Funct. Mater.* **2011**, *21*, 501−509.
(31) Pan, Y.; Du, X.; Zhao, F.; Xu, B. Magnetic Nanoparticles for the Manipulation of Proteins and Cells. *Chem. Soc. Rev.* **2012**, *41*, 2912−2942.
(32) Kim, J.; Kim, H. S.; Lee, N.; Kim, T.; Kim, H.; Yu, T.; Song, I. C.; Moon, W. K.; Hyeon, T. Multifunctional Uniform Nanoparticles Composed of a Magnetite Nanocrystal Core and a Mesoporous Silica Shell for Magnetic Resonance and Fluorescence Imaging and for Drug Delivery. *Angew. Chem., Int. Ed.* **2008**, *47*, 8438−8441.
(33) Gijs, M. A.; Lacharme, F. d. r.; Lehmann, U. Microfluidic Applications of Magnetic Particles for Biological Analysis and Catalysis. *Chem. Rev.* **2010**, *110*, 1518−1563.
(34) Li, Y.; Hu, Y.; Jiang, H.; Li, C. Double-faced γ-Fe $_2$ O $_3$|| SiO_2 Nanohybrids: Flame Synthesis, in Situ Selective Modification and Highly Interfacial Activity. *Nanoscale* **2013**, *5*, 5360−5367.
(35) Chen, Z.; Yin, J.-J.; Zhou, Y.-T.; Zhang, Y.; Song, L.; Song, M.; Hu, S.; Gu, N. Dual Enzyme-like Activities of Iron Oxide Nanoparticles and their Implication for Diminishing cytotoxicity. *ACS Nano* **2012**, *6*, 4001−4012.
(36) Wang, F.; Pauletti, G. M.; Wang, J.; Zhang, J.; Ewing, R. C.; Wang, Y.; Shi, D. Dual Surface-Functionalized Janus Nanocomposites of Polystyrene/Fe_3O_4@SiO_2 for Simultaneous Tumor Cell Targeting and Stimulus-Induced Drug Release. *Adv. Mater.* **2013**, *25*, 3485−3489.
(37) Reddy, L. H.; Arias, J. L.; Nicolas, J.; Couvreur, P. Magnetic Nanoparticles: Design and Characterization, Toxicity and Biocompatibility, Pharmaceutical and Biomedical Applications. *Chem. Rev.* **2012**, *112*, 5818−5878.
(38) Josephy, P. D.; Eling, T.; Mason, R. P. The Horseradish Peroxidase-Catalyzed Oxidation of 3,5,3′,5′-Tetramethylbenzidine. Free Radical and Charge-Transfer Complex Intermediates. *J. Biol. Chem.* **1982**, *257*, 3669−3675.
(39) Dong, Y.-l.; Zhang, H.-g.; Rahman, Z. U.; Su, L.; Chen, X.-j.; Hu, J.; Chen, X.-g. Graphene Oxide−Fe $_3$ O $_4$ Magnetic Nanocomposites with Peroxidase-like Activity for Colorimetric Detection of Glucose. *Nanoscale* **2012**, *4*, 3969−3976.
(40) Sun, X.; Guo, S.; Chung, C. S.; Zhu, W.; Sun, S. A Sensitive H_2O_2 Assay Based on Dumbbell-like PtPd-Fe_3O_4 Nanoparticles. *Adv. Mater.* **2013**, *25*, 132−136.
(41) Lian, J.; Duan, X.; Ma, J.; Peng, P.; Kim, T.; Zheng, W. Hematite (α-Fe_2O_3) with Various Morphologies: Ionic Liquid-Assisted Synthesis, Formation Mechanism, and Properties. *ACS Nano* **2009**, *3*, 3749−3761.
(42) Asati, A.; Santra, S.; Kaittanis, C.; Nath, S.; Perez, J. M. Oxidase-Like Activity of Polymer-Coated Cerium Oxide Nanoparticles. *Angew. Chem., Int. Ed.* **2009**, *48*, 2308−2312.
(43) Wei, H.; Wang, E. Fe_3O_4 Magnetic Nanoparticles as Peroxidase Mimetics and their Applications in H_2O_2 and Glucose Detection. *Anal. Chem.* **2008**, *80*, 2250−2254.
(44) Xu, Y.; Pehrsson, P. E.; Chen, L.; Zhang, R.; Zhao, W. Double-Stranded DNA Single-Walled Carbon Nanotube Hybrids for Optical Hydrogen Peroxide and Glucose Sensing. *J. Phys. Chem. C* **2007**, *111*, 8638−8643.

DOI: 10.1021/acsami.5b03423
ACS Appl. Mater. Interfaces 2015, 7, 15395−15402